Supplemental Information

mRNA Location and Translation Rate Determine Protein Targeting to Dual Destinations

Alexander N. Gasparski, Konstadinos Moissoglu, Sandeep Pallikkuth, Sezen Meydan, Nicholas R. Guydosh and Stavroula Mili

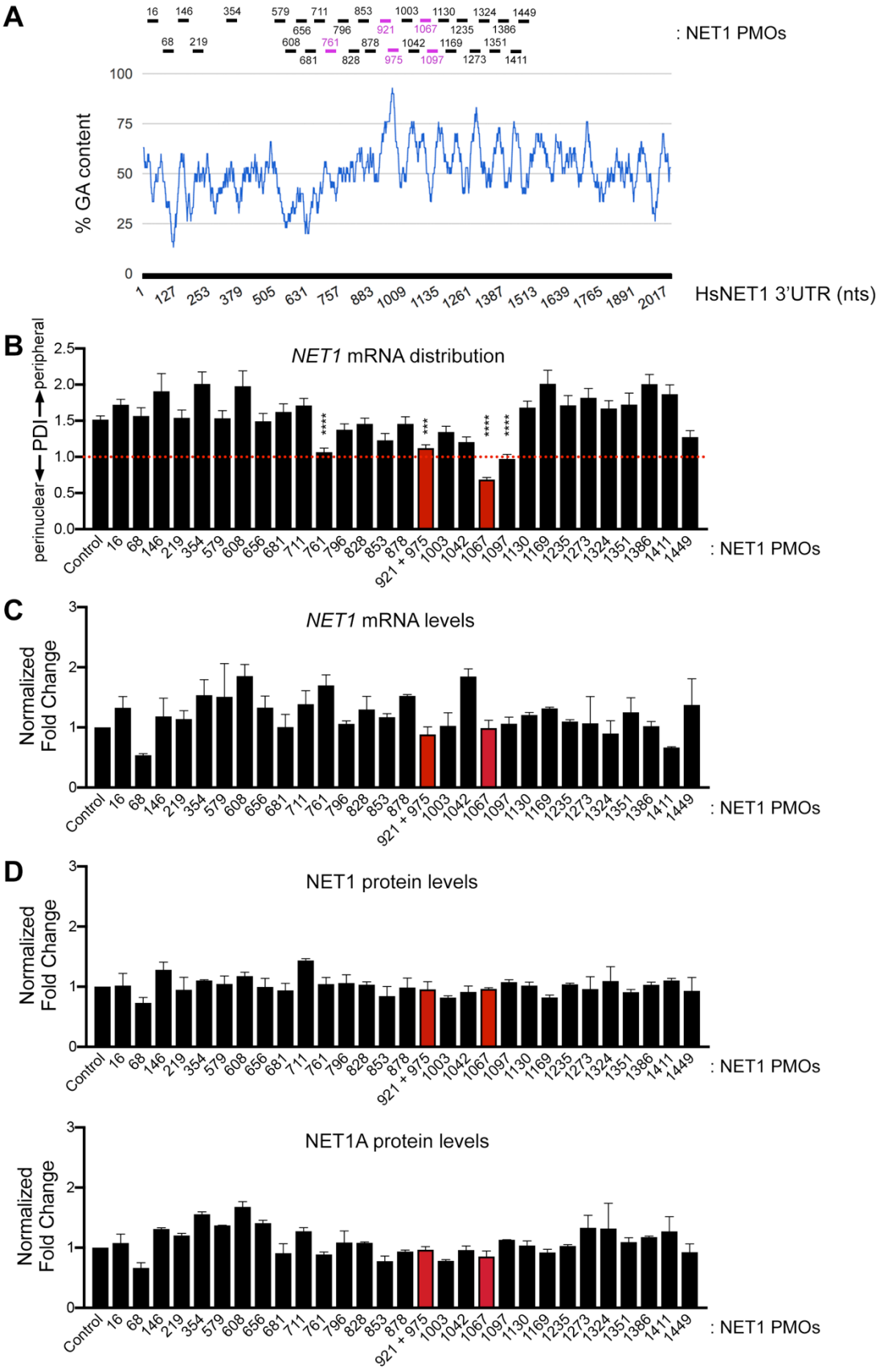
A
: NET1 PMOs
% GA content
HsNET1 3'UTR (nts)
B
NET1 mRNA distribution
perinuclear ← PDI → peripheral
: NET1 PMOs
C
NET1 mRNA levels
Normalized Fold Change
: NET1 PMOs
D
NET1 protein levels
Normalized Fold Change
: NET1 PMOs
NET1A protein levels
Normalized Fold Change
: NET1 PMOs

Figure S1: Antisense oligonucleotide tiling across the 3' UTR of the *NET1* mRNA. Related to Figure 1. (A) Chart showing the percent GA nucleotide content within the 3' UTR of the human *NET1* mRNA. The NET1 PMOs tested are shown above the chart and the PMOs in magenta are those that showed significant reduction in PDI (see B). **(B)** PDI quantification of *NET1* mRNA distribution determined by FISH of cells treated with the indicated PMOs. n=30-118 cells. PDI=1 indicates a diffuse distribution, PDI>1 indicates peripheral distribution, PDI<1 indicates a perinuclear distribution. **(C)** *NET1* mRNA levels determined by ddPCR after treatment with the indicated PMOs. n=2. **(D)** Protein levels of the NET1 and NET1A isoforms, by Western blot of cells treated with the indicated PMOs. n=2. Error bars: SEM. p-values: ***<0.001, ****<0.0001 by one-way ANOVA. The red bars indicate the *NET1* mislocalizing oligonucleotides used throughout this study.

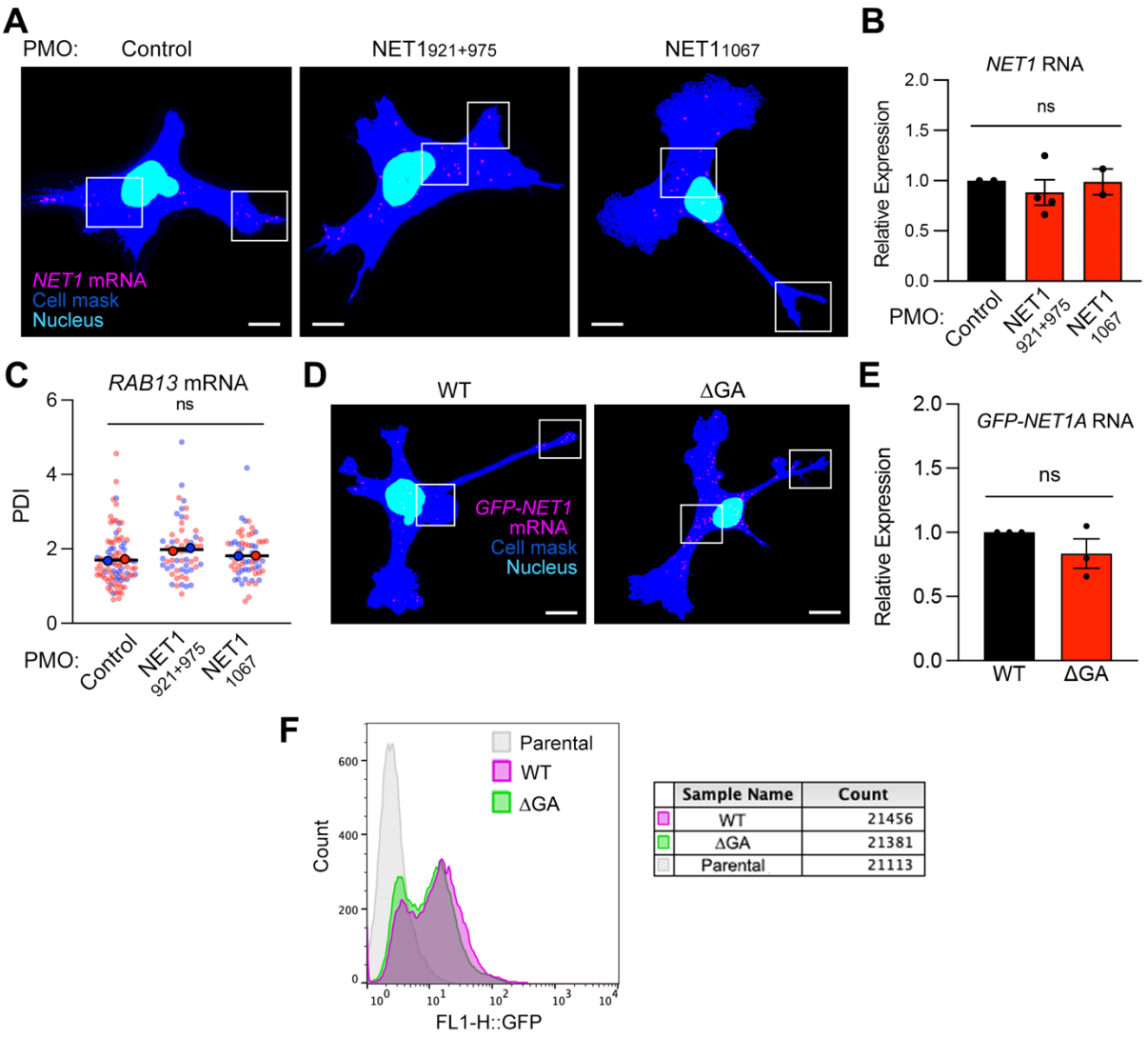

Figure S2: Specificity and effect of altering *NET1* mRNA localization on mRNA levels and protein expression. Related to Figure 1. (A) Representative RNA FISH images of MDA-MB-231 cells treated with the indicated PMOs. Boxed regions indicate areas shown in Figure 1A. **(B)** *NET1* mRNA expression measured by ddPCR of PMO treated cells. n=2-4. **(C)** PDI quantification of *RAB13* mRNA distribution in cells treated with the indicated PMOs. NET1-targeted PMOs do not alter the distribution of the co-regulated *RAB13* mRNA. **(D)** Representative RNA FISH images of cells expressing the WT and ΔGA GFP-NET1A constructs. Boxed regions indicate areas shown in Figure 1D. **(E)** *GFP-NET1A* mRNA expression as measured by ddPCR of the indicated stable cell lines. n=3. **(F)** Flow cytometry analysis of GFP fluorescence in parental MDA-MB-231 cells

and GFP-NET1A cells with either the WT or ΔGA UTR. Error bars: SEM. ns: not significant by one-way ANOVA (B, C) or unpaired t-test (E).

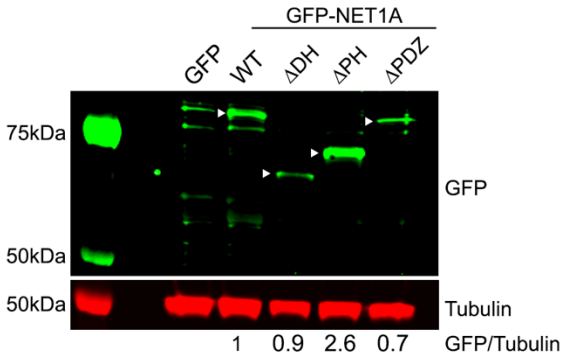

Figure S3: Characterization of GFP-NET1A mutant variants. Related to Figure 3. Western blot of stable cell lines expressing GFP or the indicated GFP-tagged NET1A variants. White arrowheads indicate the band of interest for each lane. Tubulin was used as a loading control and relative expression levels are indicated at the bottom.

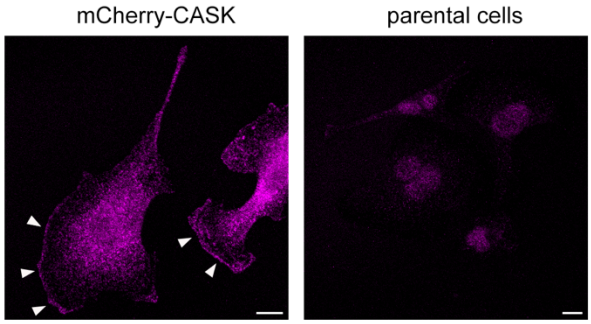

Figure S4: Intracellular CASK distribution. Related to Figure 4. Immunofluorescence of mCherry-CASK expressing cells. Arrowheads indicate peripheral areas of CASK accumulation, potentially reflecting sites of CASK association with membranes.

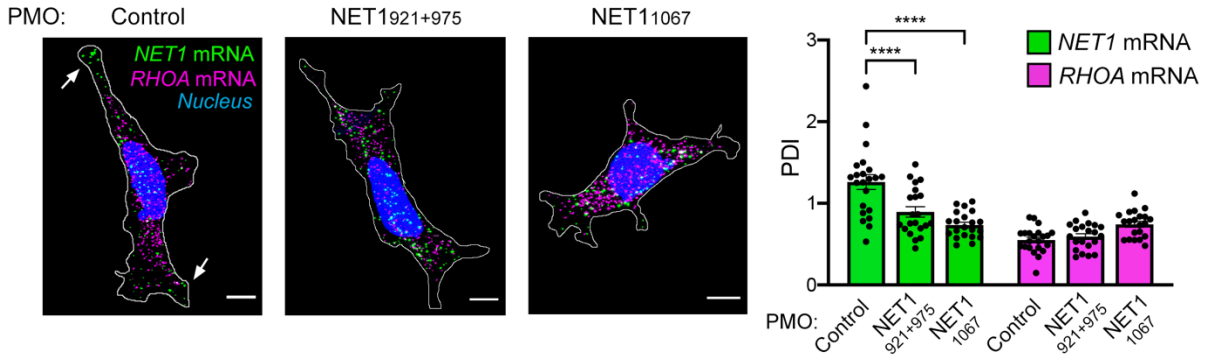

Figure S5: *NET1* mRNA localization in HEK293 cells depends on GA-rich sequences in the 3'UTR. Related to Figure 5. Representative RNA FISH images of HEK293 cells treated for 72hrs with the indicated PMOs and PDI quantification. n=21 cells. Error bars: SEM. p-values: ****<0.0001 by one-way ANOVA. Arrows indicate *NET1* mRNA localized at peripheral protrusions. NET1-targeting PMOs prevent peripheral localization of *NET1* mRNA, but do not alter the distribution of *RHOA* mRNA. Scale bars: 10μm.

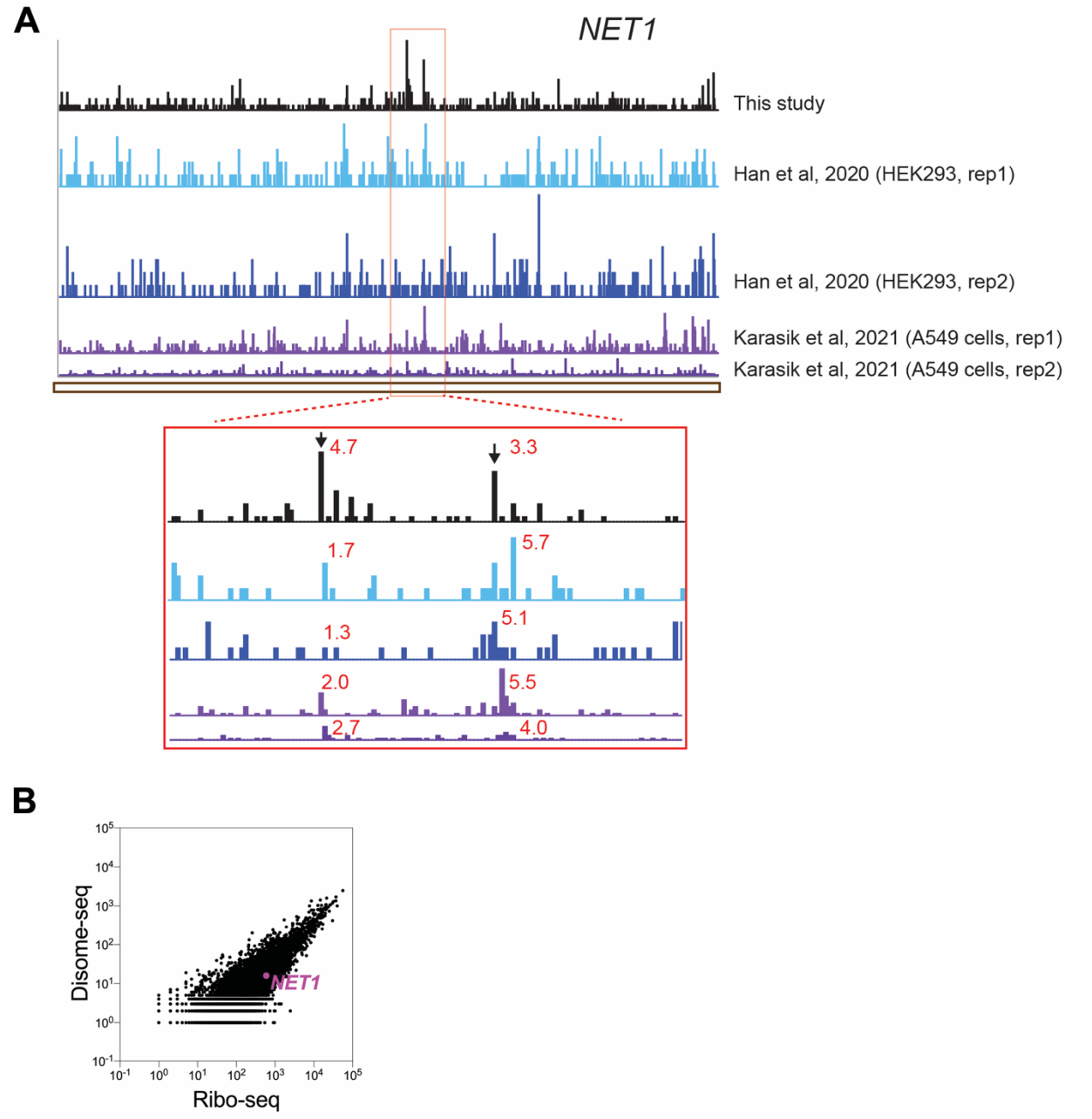

Figure S6: **Ribosome profiling data of the NET1 transcript. Related to Figure 5. (A)** Snapshot of Ribo-seq reads mapped to the NET1 transcript in different datasets. Magnified inset at the bottom shows the reproducibility of both stalling peaks. The numbers in red next to each stalling peak indicate the pause score, which is calculated by averaging the reads -/+ 5 nt of the stalling peak and dividing that number to the average reads mapped to NET1 coding region. **(B)** Comparison of raw Disome-seq and Ribo-seq reads. NET1 is highlighted, where the number of Disome-seq and Ribo-seq reads mapped to NET1 are 16 and 591, respectively.

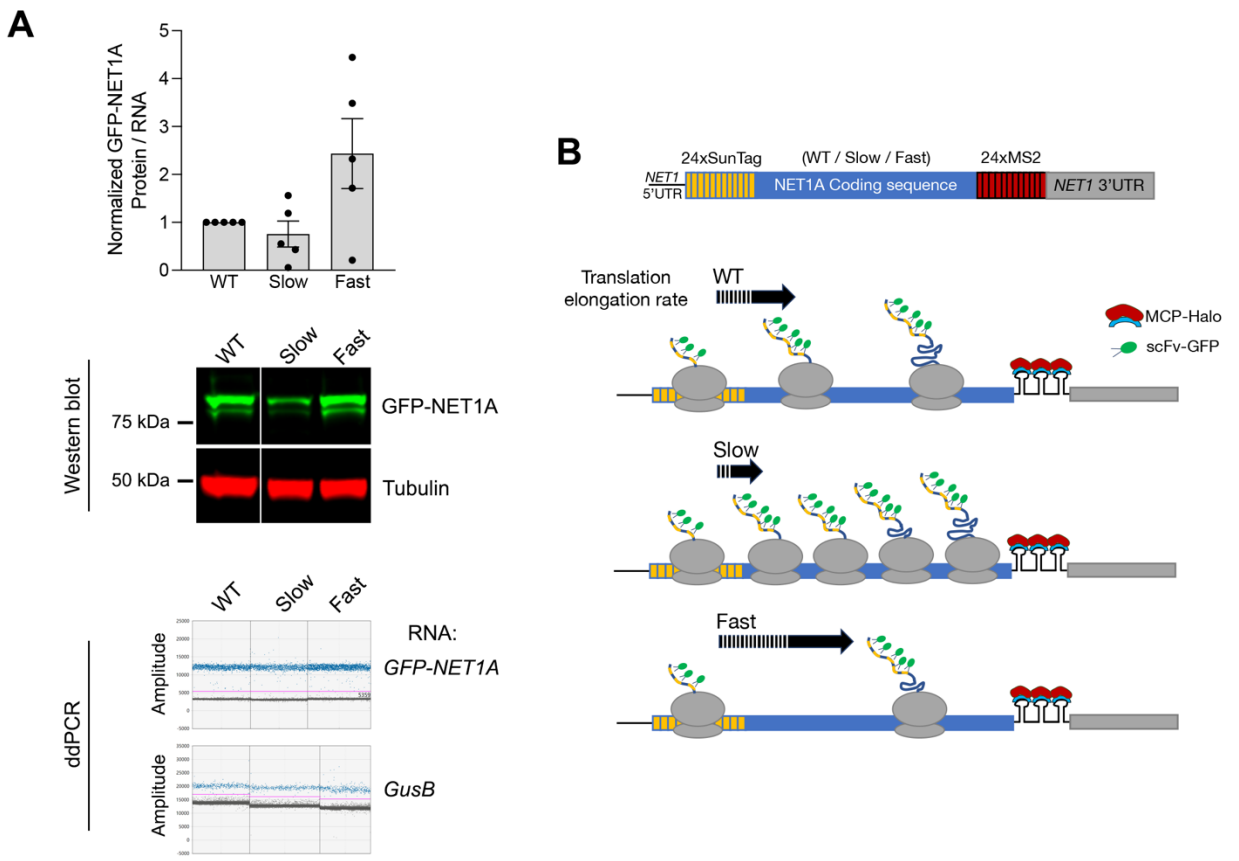

Figure S7: NET1A mutants with altered translation elongation rates. Related to Figure 5. **(A)** Normalized GFP-NET1A protein/RNA ratio for the indicated stable GFP-NET1A-expressing cell lines (wild type (WT), slow or fast). Protein levels determined by Western blot; RNA levels by ddPCR. Representative results are shown in respective panels underneath the graph. Tubulin protein and *GusB* RNA were used as normalization controls. Error bars: SEM **(B)** Upper: schematic of overall structure of reporter constructs used for single-molecule translation site imaging. Reporters contain the 5'- and 3'-UTR sequences of human *NET1*, the wild type NET1 coding sequence (or slow and fast mutant variants), and 24 copies of SunTag epitopes and MS2 binding sites, used for fluorescence imaging detection. Lower: Schematic predictions of changes in ribosome occupancy per mRNA induced by the indicated changes in translation elongation rates.

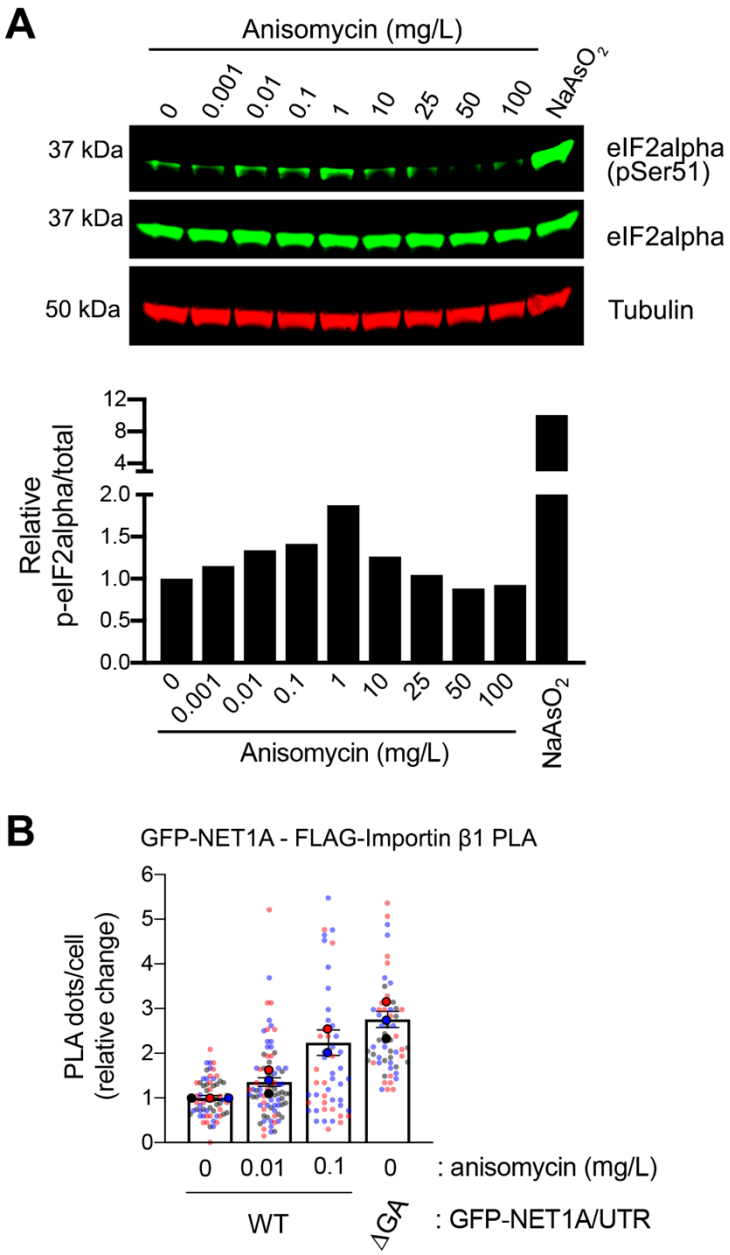

Figure S8: Sub-inhibitory concentrations of anisomycin increase interaction of NET1A with importin. Related to Figure 5. (A) Western blot and quantification of pSer51-eIF2α levels in MDA-MB-231 cells treated with the indicated concentrations of anisomycin for 30min. For comparison, cells were treated with sodium arsenite for 30 min. **(B)** Quantification of in situ interaction between GFP-NET1A and FLAG-importin β1, by PLA of the indicated cell lines expressing GFP-NET1A from a peripheral (WT) or perinuclear RNA (ΔGA). n=52-80 in 2-3 independent experiments. In superplot, data points from individual replicates are color coded, and large, outlined color dots indicate the mean of each replicate. Error bars: SEM.

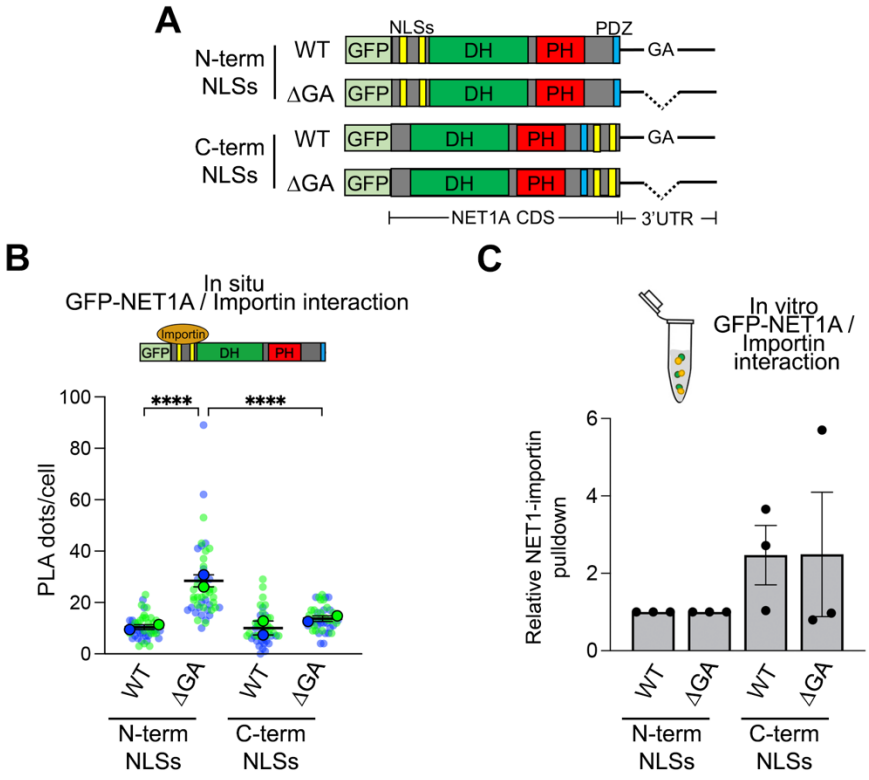

Figure S9: Order of NLS appearance influences NET1-importin interaction. Related to Figure 5. (A) Schematic of GFP-NET1A constructs used for generation of stably expressing MDA-MB-231 cell lines. The normally occurring N-terminal NLSs were transferred to the C-terminus, thus being synthesized after the PH domain. Variants were expressed from transcripts carrying either the WT 3'UTR or a mutant with a deletion of the GA-rich region. **(B)** Quantification of in situ interaction between GFP-NET1A and FLAG-importin β1, by PLA of the indicated cell lines. n=45-49 from 2 independent experiments. **(C)** Quantification of relative pulldown efficiency of GFP-NET1A from lysates of the indicated cell lines with GST-importin α5. n=2. In superplots, data points from individual replicates are color coded, and large, outlined color dots indicate the mean of each replicate. Error bars: SEM. p-values: ****<0.0001, one-way ANOVA.

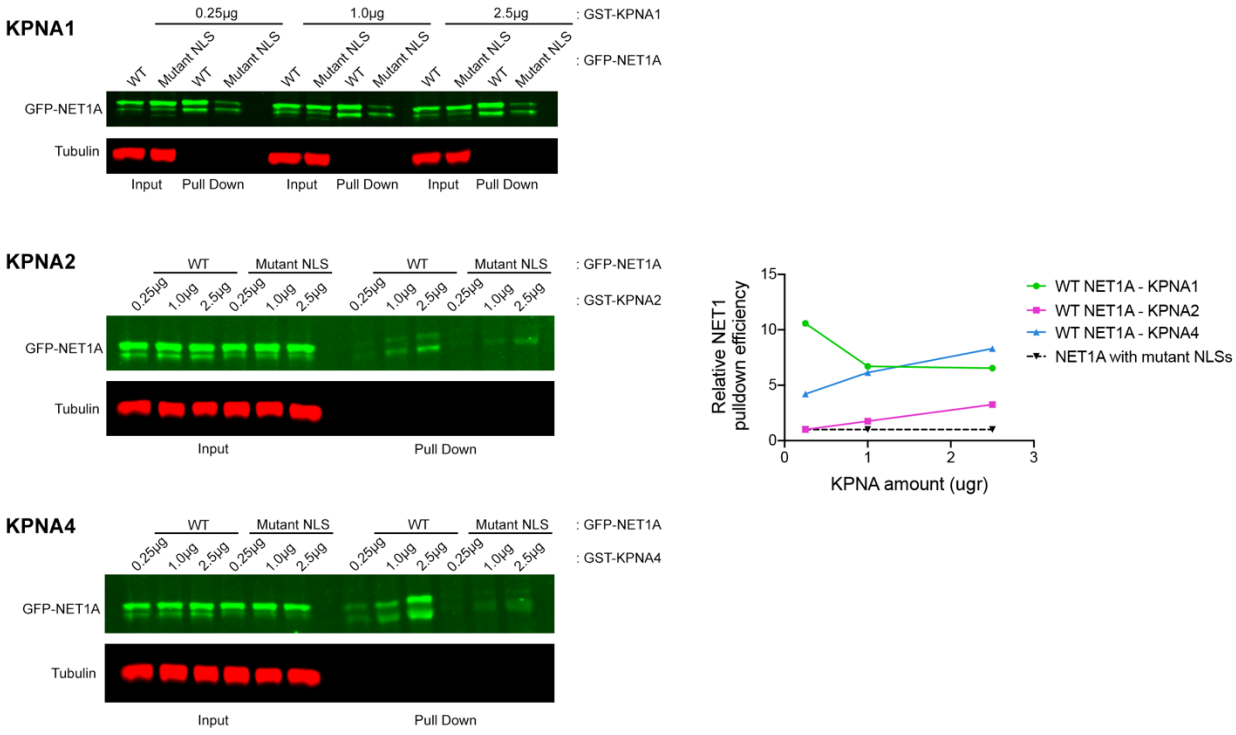

Figure S10: In vitro GFP-NET1A-importin α interaction. Related to Figure 5. The indicated amounts of GST-importin α members (GST-KPNA1, GST-KPNA2, GST-KPNA4) were used for pulldown assays with lysates of GFP-NET1A-expressing cells. Pulldown efficiency is plotted relative to NLS mutant GFP-NET1A. GST-KPNA1 exhibits efficient binding at all concentrations tested and was used for further experiments.

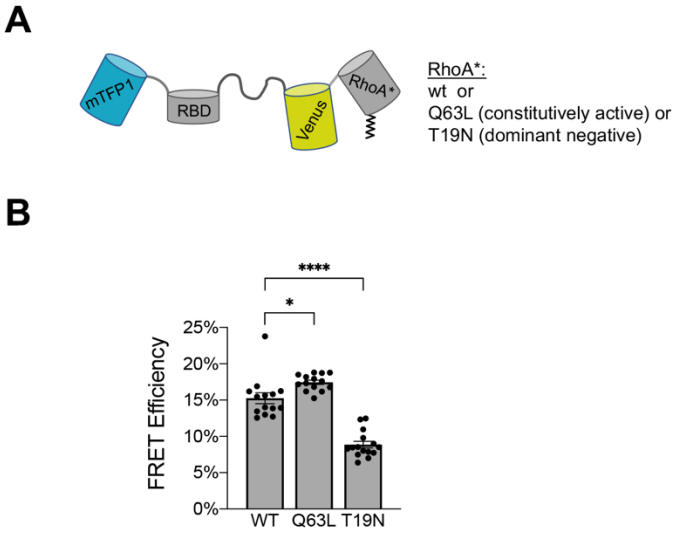

Figure S11: Validation of RhoA FRET biosensor. Related to Figure 6. (A) Schematic of the biosensor used for RhoA activity estimation. **(B)** FRET efficiency measurements from a biosensor carrying wt RhoA, Q63L RhoA (constitutively active), or T19N RhoA (dominant negative). The biosensor can distinguish different levels of RhoA activity. Error bars: SEM. p-values: *<0.05, ****<0.0001 by one-way ANOVA.

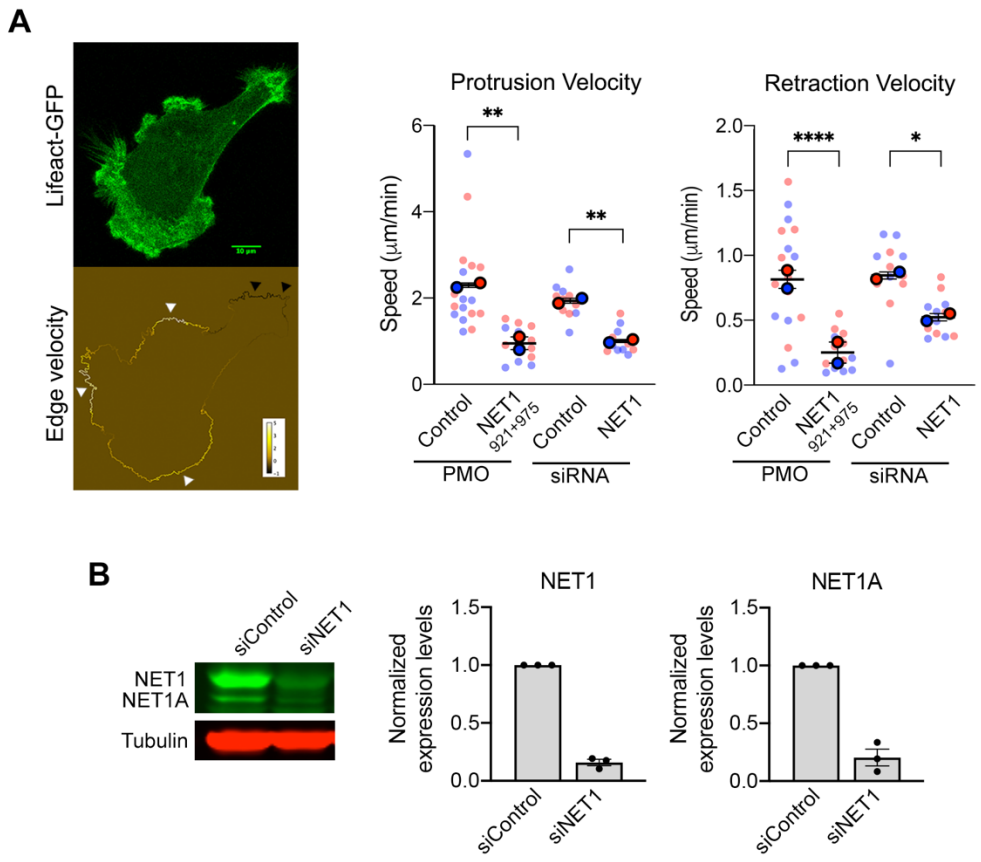

Figure S12: Peripheral *NET1* mRNA localization is essential for NET1 function in membrane edge dynamics. Related to Figure 6. (A) Membrane protrusion and retraction speeds were measured in Lifeact-GFP cells treated with the indicated PMOs or siRNAs. Average protrusion and retraction velocities were calculated using an automated script. Image panels (left) show snapshots of time lapse movie (upper) and analysis output (bottom). The script measures edge velocity (protrusion: white arrowheads and retraction: black arrowheads) between consecutive frames of each time lapse movie and calculates average values for each analyzed cell. n=12-17 cells from two independent biological replicates. Error bars: SEM. p-values: *<0.05, **<0.01, ****<0.0001 by one-way ANOVA. Scale bar = 10um. **(B)** Western blot analysis of NET1 and NET1A protein levels upon siRNA treatment.

Table S1: Sequences of coding region fragments used for generation of plasmid constructs. Related to STAR Methods.

WT NET1A: Coding Sequence
gtggcacatgatgagactggaggtctcctacctattaaaaggaccatacgagtcctagatgtcaataaccagtccttcagagaacaa gaggagccaagcaataaaagagttcgacctctggctcgtgtcacgtccttggcaaatttaatctctcctgtaagaaatggagctgtca gacgttttggtcaaacaatacagtcatttacccttcgtggtgaccacagatccccagcctctgcccagaagttttctagcaggtcaaca gtcccaacacccgccaagagaaggagcagtgcactgtggtcagagatgctggacatcaccatgaaggagtctctcaccaccaggga gatcagacggcaggaggcaatatatgaaatgtcccgaggtgaacaggatttaattgaggatctcaaacttgcaagaaaggcctacc atgaccccatgttaaagttgtccatcatgtcagaagaggaactcacacatatatttggtgatctggactcttacatacctctgcatgaa gatttgttgacaagaataggagaagcaaccaagcctgatggaacagtggagcagattggtcacattctcgtgagctggttaccgcgc ttgaatgcctacagaggttactgtagtaaccagctggcagccaaagctcttcttgatcaaaagaaacaggatccaagagtccaagac ttcctccagcgatgtctcgagtctcccttcagtcgaaaactagatctttggagtttcctagatatccctcgaagtcgcctagtcaaatacc ctttactgttaaaagaaattcttaaacacactccaaaagagcaccctgatgttcagcttctggaggatgctatattgataatacaggga gtcctctctgatatcaacttgaagaaaggtgaatccgagtgccagtattacatcgacaagctggagtacctggatgaaaagcagagg gaccccagaatcgaagcgagcaaagtgctgctgtgccatggggagctgcggagcaagagtggacataaactttacattttcctgtttc aagacatcttggttctgactcggcccgtcacacggaacgaacggcactcttaccaggtttaccggcagccaatcccagtccaagagct agtcctagaagacctgcaggatggagatgtgagaatgggaggctcctttcgaggagctttcagtaactcagagaaagctaaaaatat ctttagaattcgcttccatgacccctctccagcccagtctcacactctgcaagccaatgacgtgttccacaagcagcagtggttcaact gtattcgagcggccattgccccctttccagtcggcaggcagtccacctgagctgcagggcctgccggagctgcacgaagagtgtgagg ggaaccacccctctgcgaggaaactcacagcccagaggagggcatccacagtttccagtgttactcaggtagaagttgatgaaaacg cttacagatgtggctctggcatgcagatggcagaggacagcaagagcttaaagacacaccagacacagcccggcatccgaagagc gagggacaaagccctttctggtggcaaacggaaagagactttggtgtag
Slow Mutant: NET1A coding sequence shown (region highlighted contains mutations to introduce suboptimal codons)
gtggcacatgatgagactggaggtctcctacctattaaaaggaccatacgagtcctagatgtcaataaccagtccttcagagaacaa gaggagccaagcaataaaagagttcgacctctggctcgtgtcacgtccttggcaaatttaatctctcctgtaagaaatggagctgtca gacgttttggtcaaacaatacagtcatttacccttcgtggtgaccacagatccccagcctctgcccagaagttttctagcaggtcaaca gtcccaacacccgccaagagaaggagcagtgcactgtggtcagagatgcttgacataacgatgaaggagtctttgacgacgaggga gataagacggcaggaggcgatatatgaaatgtcacgaggtgaacaagatttaattgaggatctaaaacttgcgagaaaggcgtacc atgacccgatgttaaagttgtccataatgtcagaagaggaactaacacatatatttggtgatctagactcttacatacctcttcatgaa gatttgttgacaagaataggtgaagcgacgaagccggatggtacagtagagcaaataggtcacatactcgttagctggttaccgcgc ttgaatgcgtacagaggttactgtagtaaccagttggcagccaaagctcttcttgatcaaaagaaacaggatccaagagtccaagac ttcttgcagcgatgtttggagtctcccttcagtcgaaaactagatctttggagtttcctagatataccgcgaagtcgcctagtcaaatac ccgttactgttaaaagaaattcttaaacacactccaaaagagcaccctgatgttcagcttctcgaggatgcgatattgataatacaag gagtcctctctgatataaacttgaagaaaggtgaatccgagtgccaatattacatagacaagcttgagtacctagatgaaaagcaga gggaccccagaatagaagcgagcaaagtgttgctttgccatggggagctgcggagcaagagtggacataaactttacattttcctgtt tcaagacatcttggttctgactcggcccgtcacacggaacgaacggcactcttaccaggtttaccggcagccaatcccagtccaagag ctagtcctagaagacctgcaggatggagatgtgagaatgggaggctcctttcgaggagctttcagtaactcagagaaagctaaaaat atctttagaattcgcttccatgacccctctccagcccagtctcacactctgcaagccaatgacgtgttccacaagcagcagtggttcaa ctgtattcgagcggccattgccccctttccagtcggcaggcagtccacctgagctgcagggcctgccggagctgcacgaagagtgtgag gggaaccacccctctgcgaggaaactcacagcccagaggagggcatccacagtttccagtgttactcaggtagaagttgatgaaaac

gcttacagatgtggctctggcatgcagatggcagaggacagcaagagcttaaagacacaccagacacagcccggcatccgaagag
cgagggacaaagccctttctggtggcaaacggaaagagactttggtgtag

Fast mutant: NET1A coding sequence shown (regions highlighted contain the mutations of the identified stall sites)

gtggcacatgatgagactggaggtctcctacctattaaaaggaccatacgagtcctagatgtcaataaccagtccttcagagaacaa
gaggagccaagcaataaaagagttcgacctctggctcgtgtcacgtccttggcaaatttaatctctcctgtaagaaatggagctgtca
gacgttttggtcaaacaatacagtcatttacccttcgtggtgaccacagatccccagcctctgcccagaagttttctagcaggtcaaca
gtcccaacacccgccaagagaaggagcagtgcactgtggtcagagatgctggacatcaccatgaaggagtctctcaccaccaggga
gatcagacggcaggaggcaatatatgaaatgtcccgaggtgaacaggatttaattgaggatctcaaacttgcaagaaaggcctacc
atgaccccatgttaaagttgtccatcatgtcagaagaggaactcacacatatatttggtgatctggactcttacatacctctgcatgaa
gatttgttgacaagaataggagaagcaaccaagcctgatggaacagtggagcagattggtcacattctcgtgagctggttaccgcgc
ttgaatgcctacagaggttactgtagtaaccagctggcagccaaagctcttcttgatcaaaagaaacaggatccaagagtccaagac
ttcctccagcgatgtctcgagtctcccttcagtcgaaaactagatctttggagtttcctagatatccctcgaagtcgcctagtcaaaggc
ggcctgctgttaaaagaaattcttaaacacactccaaaagagcacggcggcgtgcagcttctggaggatgctatattgataatacag
ggagtcctctctgatatcaacttgaagaaaggtgaatccgagtgccagtattacatcgacaagctggagtacctggatgaaaagcag
agggaccccagaatcgaagcgagcaaagtgctgctgtgccatggggagctgcggagcaagagtggacataaactttacattttcctg
tttcaagacatcttggttctgactcggcccgtcacacggaacgaacggcactcttaccaggtttaccggcagccaatcccagtccaag
agctagtcctagaagacctgcaggatggagatgtgagaatgggaggctcctttcgaggagctttcagtaactcagagaaagctaaaa
atatctttagaattcgcttccatgacccctctccagcccagtctcacactctgcaagccaatgacgtgttccacaagcagcagtggttca
actgtattcgagcggccattgccccttccagtcggcaggcagtccacctgagctgcagggcctgccggagctgcacgaagagtgtga
ggggaaccacccctctgcgaggaaactcacagcccagaggagggcatccacagtttccagtgttactcaggtagaagttgatgaaa
acgcttacagatgtggctctggcatgcagatggcagaggacagcaagagcttaaagacacaccagacacagcccggcatccgaag
agcgagggacaaagccctttctggtggcaaacggaaagagactttggtgtag

Mutant NLS: NET1A coding sequence shown (regions highlighted contain mutations of amino acids within two basic NLSs):

gtggcacatgatgagactggaggtctcctacctattaaaaggaccatacgagtcctagatgtcaataaccagtccttcagagaacaa
gaggagccaagcaatgccgccgttgcccctctggctcgtgtcacgtccttggcaaatttaatctctcctgtaagaaatggagctgtcag
acgttttggtcaaacaatacagtcatttacccttcgtggtgaccacagatccccagcctctgcccagaagttttctagcaggtcaacagt
cccaacacccgccgctgctgccagcagtgcactgtggtcagagatgctggacatcaccatgaaggagtctctcaccaccagggagat
cagacggcaggaggcaatatatgaaatgtcccgaggtgaacaggatttaattgaggatctcaaacttgcaagaaaggcctaccatg
accccatgttaaagttgtccatcatgtcagaagaggaactcacacatatatttggtgatctggactcttacatacctctgcatgaagatt
gttgacaagaataggagaagcaaccaagcctgatggaacagtggagcagattggtcacattctcgtgagctggttaccgcgcttga
atgcctacagaggttactgtagtaaccagctggcagccaaagctcttcttgatcaaaagaaacaggatccaagagtccaagacttcct
ccagcgatgtctcgagtctcccttcagtcgaaaactagatctttggagtttcctagatatccctcgaagtcgcctagtcaaataccctttt
actgttaaaagaaattcttaaacacactccaaaagagcaccctgatgttcagcttctggaggatgctatattgataatacagggagtc
ctctctgatatcaacttgaagaaaggtgaatccgagtgccagtattacatcgacaagctggagtacctggatgaaaagcagagggac
cccagaatcgaagcgagcaaagtgctgctgtgccatggggagctgcggagcaagagtggacataaactttacattttcctgtttcaag
acatcttggttctgactcggcccgtcacacggaacgaacggcactcttaccaggtttaccggcagccaatcccagtccaagagctagt
cctagaagacctgcaggatggagatgtgagaatgggaggctcctttcgaggagctttcagtaactcagagaaagctaaaaatatctt
tagaattcgcttccatgacccctctccagcccagtctcacactctgcaagccaatgacgtgttccacaagcagcagtggttcaactgta
ttcgagcggccattgccccttccagtcggcaggcagtccacctgagctgcagggcctgccggagctgcacgaagagtgtgagggga

accacccctctgcgaggaaactcacagcccagaggagggcatccacagtttccagtgttactcaggtagaagttgatgaaaacgctt
acagatgtggctctggcatgcagatggcagaggacagcaagagcttaaagacacaccagacacagcccggcatccgaagagcgag
ggacaaagccctttctggtggcaaacggaaagagactttggtgtag

C-term NLS: NET1A coding sequence shown (region highlighted contains NLSs (green) and was transferred from the N-terminus to the C-terminus of the protein):

tggtcagagatgctggacatcaccatgaaggagtctctcaccaccagggagatcagacggcaggaggcaatatatgaaatgtcccg
aggtgaacaggatttaattgaggatctcaaacttgcaagaaaggcctatcatgaccccatgttaaagttgtccatcatgtcagaagag
gaactcacacatatatttggtgatctggactcttacatacctctgcatgaagatttgttgacaagaataggagaagcaaccaagcctg
atggaacagtggagcagattggtcacattctcgtgagctggttaccgcgcttgaatgcctacagaggttactgtagtaaccagctggc
agccaaagctcttcttgatcaaaagaaacaggatccaagagtccaagacttcctccagcgatgtctcgagtctcccttcagtcgaaaa
ctagatctttggagtttcctagatatccctcgaagtcgcctagtcaaataccctttactgttaaaagaaattcttaaacacactccaaaa
gagcaccctgatgttcagcttctggaggatgctatattgataatacagggagtcctctctgatatcaacttgaagaaaggtgaatccga
gtgccagtattacatcgacaagctggagtacctggatgaaaagcagagggaccccagaatcgaagcgagcaaagtgctgctgtgcc
atggggagctgcggagcaagagtggacataaactttacattttcctgtttcaagacatcttggttctgactcggcccgtcacacggaac
gaacggcactcttaccaggtttaccggcagccaatcccagtccaagagctagtcctagaagacctgcaggatggagatgtgagaatg
ggaggctcctttcgaggagctttcagtaactcagagaaagctaaaaatatctttagaattcgcttccatgacccctctccagcccagtc
tcacactctgcaagccaatgacgtgttccacaagcagcagtggttcaactgtattcgagcggccattgccccttccagtcggcaggc
agtccacctgagctgcagggcctgccggagctgcacgaagagtgtgaggggaaccacccctctgcgaggaaactcacagcccagag
gagggcatccacagtttccagtgttactcaggtagaagttgatgaaaacgcttacagatgtggctctggcatgcagatggcagagga
cagcaagagcttaaagacacaccagacacagcccggcatccgaagagcgagggacaaagccctttctggtggcaaacggaaaga
gactttggtgGTCGACggaccagtcgcactcGTGGCACATGATGAGACTGGAGGTCTCCTACCTATTAAAAGG
ACCATACGAGTCCTAGATGTCAATAACCAGTCCTTCAGAGAACAAGAGGAGCCAAGCAATAAAAGAG
TTCGACCTCTGGCTCGTGTCACGTCCTTGGCAAATTTAATCTCTCCTGTAAGAAATGGAGCTGTCAGAC
GTTTTGGTCAAACAATACAGTCATTTACCCTTCGTGGTGACCACAGATCCCCAGCCTCTGCCCAGAAGT
TTTCTAGCAGGTCAACAGTCCCAACACCCGCCAAGAGAAGGAGCAGTGCACTGTAA

Table S2: Sequences of morpholino oligonucleotides (PMOs). Related to STAR Methods.

PMO name	Sequence
Control	cctcttacctcagttacaatttata
NET1-16	aacaaacagtctctcccatcagtta
NET1-68	gtaaccctatgatgctccccttacg
NET1-146	atctgtatatctttagctgccatta
NET1-219	ataccaggcttaccatgttctaaat
NET1-354	actggcagaattccagcatttgcaa
NET1-579	aaataatcggcaggttaaatgaatg
NET1-608	gctaaaaactactttacaataaaaa
NET1-656	agacatgccaatttgaaaaggcatc
NET1-681	ttaatcaggaagaaaaatactttaa
NET1-711	acacacacacacacacatacacaca
NET1-761	cttggtttcacttggtaaaattaat
NET1-796	tggcaattttcttaattggctcaaa
NET1-828	ggtctttaccctgaaatgctacact
NET1-853	ctagaatacatcaagccatttcatg
NET1-878	tttgaagtggttttctttcagtagt
NET1-921	tccctcttgcatttcagacaacact
NET1-975	gacaaaactactctcttttcctctc
NET1-1003	tctggcacaaccagacattttactt
NET1-1042	agttgagcttctcctatctcctttc
NET1-1067	ttctacaacttactacacgccctca
NET1-1097	aaggcaaataagtccacgtcccctc
NET1-1130	tttcaaactcattatttgcaggtat
NET1-1169	tctaatatggtcaaatttttaacac
NET1-1235	gaaacattttgtaataaaagattca
NET1-1273	tcctccccccctttcaaagatgatga
NET1-1324	atagtcaacactgacttgaattgat
NET1-1351	ttccactggccaaatatatttcaca
NET1-1386	ggatggatctatttacagtcttttc
NET1-1411	attcatttgtacagagaaatcattt
NET1-1449	gtgattatgtgtgtgctttttttt